# Antiferromagnetic order and frustration in small clusters

E. Viitala, J. Merikoski, M. Manninen, and J. Timonen
*Department of Physics, University of Jyväskylä, P.O. Box 35, FIN-40351 Jyväskylä, Finland*
(Received 9 December 1996)

Magnetic properties of small antiferromagnetic clusters are studied within the framework of the nearest-neighbor Ising model. We analyze in detail several cluster geometries with different lattice structures and examine the competing effects due to antiferromagnetic order, frustration, and external field. For some geometries in the presence of an external magnetic field, magnetization is found to increase with increasing temperature in a considerable temperature range. We also consider conditions under which antiferromagnetic clusters can display superparamagnetic behavior. In general, magnetization is found to depend strongly on the lattice structure of the cluster, but to be rather insensitive to local modifications of the coupling strength. The approach towards the bulk properties for increasing cluster size and the possibility of deducing the lattice structure from the observed magnetic behavior are discussed. [S0163-1829(97)08517-2]

## I. INTRODUCTION

The magnetic properties of atomic clusters have attracted intense experimental, practical, and theoretical interest recently.[1–4] The effects of finite size and reduced dimensionality appear to play the key role for clusters with size up to several hundred atoms. The experimental results for small ferromagnetic iron[5] and cobalt[6] clusters can mostly be understood within the framework of a simple superparamagnetic model.[2,3] The most unexpected feature of some measurements has been the reported *increase* in magnetization with increasing temperature.[5,7] A similar behavior of terbium clusters has been proposed to result from antiferromagnetic couplings between the atomic magnetic moments.[8] However, there has been some controversy as to the determination of the cluster temperature in the experiments,[7,9] and the physics underlying these observations is not well understood.

In this paper, we consider systematically the effects of antiferromagnetic couplings on the magnetic properties using the nearest-neighbor Ising model. Within this model, qualitative differences in magnetization between icosahedral and cuboctahedral lattice structures have already been examined by Reddy and Khanna[10] by using Monte Carlo simulations. In that work the effect of finite size on the frustration inherent in the lattice structure was found to be strongly dependent on geometry. In the present work, this picture is sharpened by a detailed study of magnetic ordering in different geometries and lattice structures. Our results for clusters up to 30 spins are obtained by numerical computations for the relevant Hamiltonians. After defining the model in Sec. II and discussing the generic features of magnetization for clusters with ideal geometry in Sec. III, we shall consider less ideal cases: We examine clusters with incomplete geometric shells in Sec. IV and effects of modified interactions for surface spins and frozen disorder in Sec. V. In addition to the case of weak external magnetic fields studied in Ref. 10, we consider in particular the behavior in the presence of a field strong enough to override the exchange energy between spins. In the antiferromagnetic case fairly large (in units of the coupling constant) values of the field can actually be appropriate, because antiferromagnetic couplings are typically weaker than the ferromagnetic ones in, e.g., the transition metals.[11] We shall be mainly concerned with the behavior at low temperatures, for which the phenomena related to antiferromagnetic ordering are most pronounced. We also discuss the possibility of a superparamagnetlike behavior in weak external fields for some cluster geometries in Sec. VI and finite-size ''transitions'' in Sec. VII. Overall, we find the magnetic properties to be strongly dependent on the lattice structure of the cluster so that no generic ''phase diagram'' for small clusters can be constructed. However, the effects of locally varying strength of the coupling constants due to surface effects and disorder seem to be less prominent. Finally, we shall discuss the experimental relevance of our conclusions in Sec. VIII.

## II. MODEL AND METHOD

We have used the nearest-neighbor Ising model,[11] where each atom labeled by $i$ in the cluster of $N$ atoms with a given geometry has a localized spin described by an Ising variable $S_i = \pm 1$. The magnetic energy of a microstate with spin configuration $\{S_i\}$ is given by

$$E(\{S_i\}) = -\sum_{\langle i,j \rangle} J_{ij} S_i S_j - g\mu_B B \sum_{i=1}^{N} S_i , \qquad (2.1)$$

where $\langle i,j \rangle$ denotes a pair of nearest neighbors, $J_{ij}$ are the coupling strengths ($J_{ij} < 0$ for antiferromagnets), and $B$ is the external magnetic field. For clusters with a constant coupling strength we have defined $J_{ij} \equiv J$, and for the other cases described in Sec. V we denote by $J$ the average of $J_{ij}$ over all couplings within the cluster. The units of temperature and external field are then fixed by the choices $J = -1$, $g\mu_B = 1$, and $k_B = 1$. In the rest of this paper $J_{ij} \equiv J$ unless stated otherwise.

Some of the studied cluster geometries are shown in Fig. 1. While icosahedra (ICO) and cuboctahedra are expected to be the most stable shapes at low temperatures,[12] also clusters with fcc, hcp, and bcc lattice structures were studied to provide further examples of the effects of lattice structure and to address the role of frustration. The number of atoms in the

 

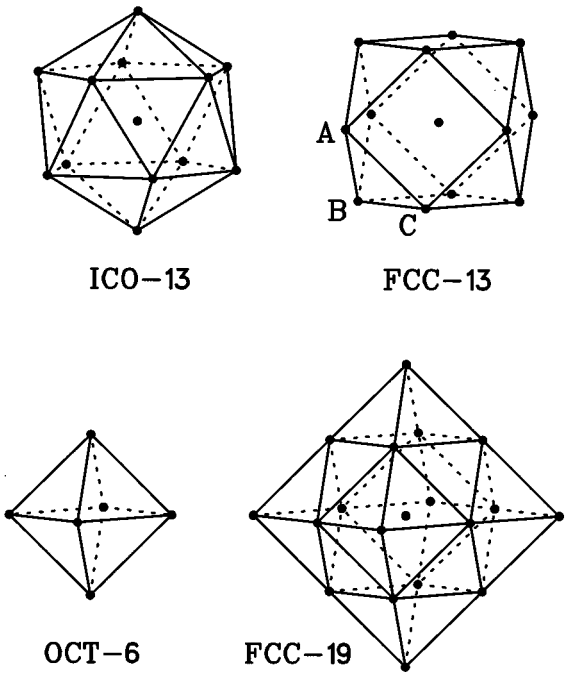


FIG. 1. Some of the cluster geometries studied in this work. All the nearest-neighbor couplings except those to the atom in the center are shown by lines.

clusters of interest varied between 6 and 30. The cluster HCP-13, where 13 is the number of atoms, can be formed from the cluster FCC-13 by rotating the triangle formed by the three atoms marked by $A$, $B$, and $C$ in Fig. 1, and by accordingly adjusting the nearest-neighbor couplings, resulting in an hcp stacking of triangular layers of atoms. Note that the cluster FCC-13 is of cuboctahedral shape and that the cluster FCC-19 is an octahedron. In Fig. 1 also the cluster OCT-6, an octahedron of six atoms, is shown. Throughout this work, we shall mean by a ''shell'' the *geometric* shell defined as a set of atoms whose distances from the center of the cluster are constant. Other kinds of definition for the shell also exist,[13] which may even be more commonly used, but they are not suitable for our purposes because we are interested in the geometrical effects on the magnetic properties. Then a cluster with ''complete shells'' is one where all lattice sites within each geometric shell of the underlying lattice up to the outermost shell are occupied by an atom. The clusters shown in Fig. 1, e.g., all have complete shells.

We have computed numerical thermodynamical averages of magnetization $M$ and absolute magnetization $|M|$ defined by

$$M=\frac{1}{N}\frac{\partial}{\partial B}[k_BT\ln Z]=\frac{1}{N}\left\langle\sum_{i=1}^{N}S_i\right\rangle, \tag{2.2}$$

$$|M|=\frac{1}{N}\left\langle\left|\sum_{i=1}^{N}S_i\right|\right\rangle, \tag{2.3}$$

where angle brackets denote ensemble average. The brute force summation over all $2^N$ Ising configurations can most conveniently be carried out by using the following algorithm. For $J_{ij}\equiv J$, the energy and consequently the probability of each microstate labeled by $r$ are determined by two integers $\epsilon_r$ and $m_r$, the energy in zero external field and the unnormalized magnetization of the spin configuration, respectively. For a given cluster geometry a two-dimensional histogram $n(\epsilon_r,m_r)$ can be formed, in which for each pair $(\epsilon_r,m_r)$ the number of configurations giving these values is saved. This histogram does not grow very large: $-N\leq m_r\leq N$ and $-N_J\leq\epsilon_r\leq N_J$, where $N_J$ is the number of nearest-neighbor couplings. Now the averages $M$ and $|M|$ can be computed at any temperature simply as a sum over the histogram. The most time-consuming task, the sorting out of the configurations into the histogram, has to be done only once for each cluster geometry. The generalization of this procedure for cases where $J_{ij}$ can have several different values is rather obvious and is not discussed here. Without exploiting any symmetries it is difficult to extend these calculations for clusters essentially larger than $N\approx 30$, because adding a new Ising spin multiplies the number of configurations and therefore the computing time by a factor of 2. The advantages of the present method are that there are no restrictions on the cluster geometry, and that the histogram itself can be used to study the details of energetics for each cluster.

By the method described above it is possible to study Ising clusters with up to $N\approx 30$ spins, while the direct numerical diagonalization of, e.g., the spin-1/2 Heisenberg Hamiltonian[11] is feasible for up to $N\approx 12$ spins. In this work clusters with Heisenberg spins have mainly been studied to examine the effects of the Ising constraints. A more detailed account of Heisenberg clusters will appear in a forthcoming publication. We have also used a simple simulated annealing procedure[14,15] to search for configurations with the lowest energy for larger Ising clusters. At low temperatures sampling of thermal fluctuations by standard equilibrium Monte Carlo simulations[15] becomes exceedingly slow. Especially for models with antiferromagnetic couplings, which turn out to have a very complicated ground-state structure, difficulties with properly weighting all meaningful parts of the configuration space appear. Therefore, in this work, sorting out all microstates of the system and averaging over all significant parts of the configuration space were chosen, while other methods were used mainly to obtain an independent check or an extension to some of the results.

## III. CLUSTERS WITH COMPLETE SHELLS

We shall first consider clusters with complete shells to examine the general behavior in high external fields. In Fig. 2 we show the magnetization $M$ at low temperatures for the clusters ICO-13, FCC-13, and HCP-13 as a function of the external magnetic field $B$. The step structure at zero temperature results from the competition between the field, which tends to align all spins in the same direction, and the antiferromagnetic coupling that favors opposite alignment between nearest-neighbor spins. (For bulk antiferromagnets this behavior is well known, and leads to the so-called field-induced transitions.[11]) In each case, the last step at $B=12$ results from flipping of the spin at the center of the cluster, while all the other spins have already become aligned with $B$. This value is needed to overcome the energy of 12 nearest-neighbor couplings. To understand the origin of the other

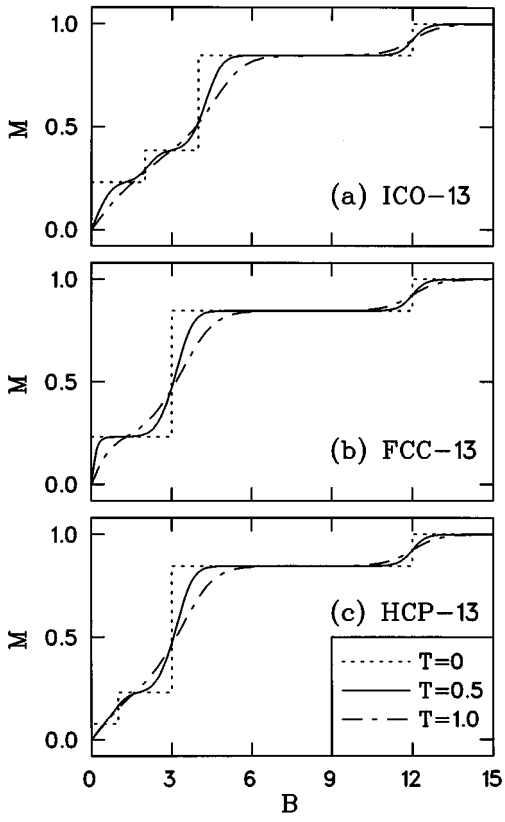


FIG. 2. Magnetization $M$ for three Ising clusters with $N=13$ as a function of the external magnetic field $B$ for three temperatures.

steps in the magnetization curves, a detailed study of the lowest-energy configurations is required. To this end, we list in Table I these configurations at $B=0$ for three cluster geometries with $N=13$. Notice that the last column in $n(\epsilon_r,m_r)$, which is the low-energy part of the histogram described in Sec. II, directly gives the degeneracy of each state. Consider now the cluster ICO-13. In the interval $0<B<2$ the ground state is, from Table I, that with $(\epsilon_r,m_r)=(-10,+3)$, and the magnetization at the first plateau in the magnetization curve at $T=0$ is $M=3/13\approx 0.23$, corresponding to energy $E=-10-3B$. In the interval $2<B<4$ the situation changes: The ground state is that with $(\epsilon_r,m_r)=(-6,+5)$, with $M=5/13\approx 0.38$ and energy $E'=-6-5B$. The step in the isotherm of Fig. 2(a) is located where the two energies coincide, $E=E'$, i.e., at $B=2$. Notice that the value $n(-12,3)=9$ for the cluster FCC-13 results from configurations of two different symmetries with degeneracies 3 and 6, of which the first one actually corresponds to the ground state of the bulk fcc antiferromagnet.

At finite temperatures the steps in the $M(B)$ curves of Fig. 2 are rounded, and curves at different temperatures can intersect each other. Therefore, magnetization is not necessarily a monotonically decreasing function of temperature, which is another feature characteristic of the antiferromagnetic case. This ''anomalous'' behavior, typical of antiferromagnetic couplings, is better seen in Fig. 3, where we show the magnetization of clusters FCC-13 and BCC-15 as a function of temperature for several values of the external field. The curve at $B=1$ for the latter cluster even has both a local minimum and a local maximum. In these figures the discrete values of $M$ possible at zero temperature provide the plateaus in the magnetization isotherms. At high temperatures the steps in the isotherms disappear, and the usual paramagnetic behavior is found. For $T\rightarrow\infty$ naturally $M\rightarrow 0$. For some values of $B$, magnetization can indeed be an increasing function of temperature for a considerable temperature range (cf. Ref. 5). In the case of the Ising model, this behavior can be understood by considering the lowest-energy spin configurations: For suitable values of $B>0$, some excited states can, due to the reduction in the antiferromagnetic order, have a larger magnetization $m_r>0$ than the ground state. We shall return to this point in Sec. VI below.

In the bcc clusters with complete shells, the spin configurations display a shell-like structure at low temperatures and in low external fields. This is due to two properties characteristic of the bcc lattice structure. First, for small clusters the coordination numbers of the spins at the same shell are the same and, second, they never have nearest neighbors at the same shell. These two conditions are sufficient for the geometrical shell structure to determine the magnetic properties. For the bcc lattice, the first condition can be shown to fail the very first time at the tenth shell of a cluster with 259 atoms. Based on this fact we conjecture that the shell structure of spin configurations of bcc clusters with complete shells pre-

TABLE I. Configurations of lowest energies at $B=0$ for three Ising clusters with $N=13$ and $J_{ij}\equiv J$. The last column $n(\epsilon_r,m_r)$ shows the number of configurations with energy $\epsilon_r$ (in units of $|J|$) and magnetization $m_r/N$.

| Cluster | $\epsilon_r$ | $m_r$ | $n(\epsilon_r,m_r)$ |
|---|---|---|---|
| ICO-13 | $-10$ | $\pm 1,\pm 3$ | 192,30 |
| | $-6$ | $\pm 1,\pm 3,\pm 5$ | 640,315,20 |
| | $-2$ | $\pm 1,\pm 3,\pm 5$ | 552,480,150 |
| FCC-13 | $-12$ | $\pm 3$ | 9 |
| | $-10$ | $\pm 1$ | 108 |
| | $-8$ | $\pm 1,\pm 3$ | 216,96 |
| HCP-13 | $-14$ | $\pm 1$ | 6 |
| | $-12$ | $\pm 1,\pm 3$ | 18,9 |
| | $-10$ | $\pm 1,\pm 3$ | 90,6 |

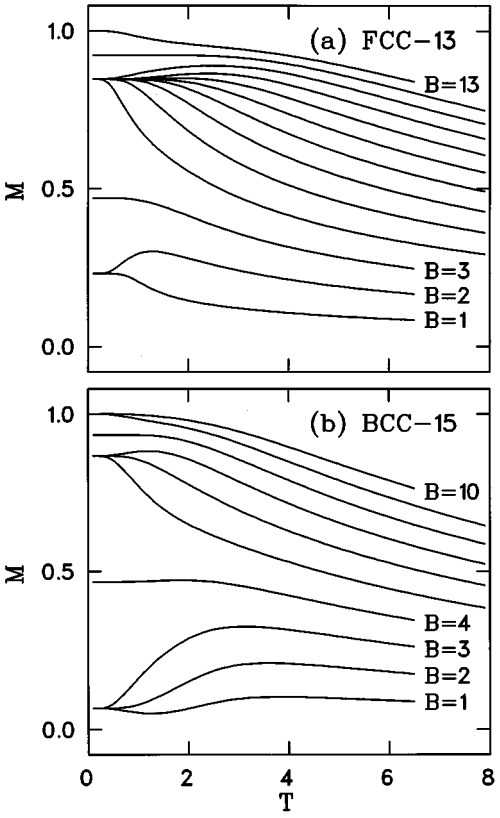


FIG. 3. Magnetization $M$ for two small Ising clusters as a function of temperature $T$ for different values of the external magnetic field $B$.

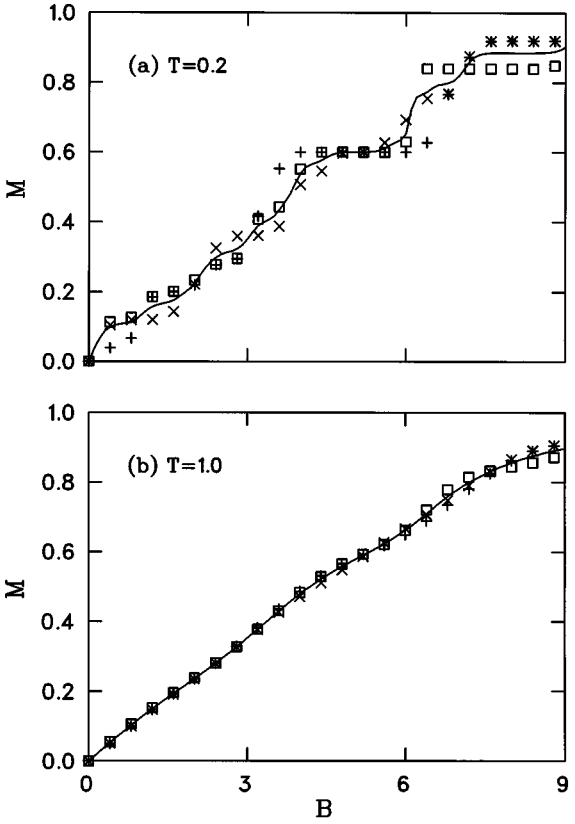


FIG. 4. Magnetizations of FCC-25 for three geometrical isomers (plotting symbols) and their average (solid curve) at two different temperatures and weighed by the appropriate degeneracy factors.

vails at least up to the cluster size of 229 atoms.

## IV. CLUSTERS WITH INCOMPLETE SHELLS

To see whether some of the magnetic properties of clusters with complete shells are not generic, we next examine clusters in which some lattice sites of the outermost shell are empty. Because cohesion dominates the total energy in real clusters, we can safely neglect the magnetic degrees of freedom in deciding which geometries to study. Then making the plausible assumption that the nearest-neighbor attraction between atoms gives the major contribution to cohesion, we can in each case concentrate on clusters with the maximum number of nearest-neighbor couplings. This does not determine the geometry uniquely, however. The fact that for a given $N$ there can be several geometries with the same average coordination number, but which cannot be transformed to each other by allowed symmetry operations, will be called *geometrical degeneracy* below. Obviously, fcc and bcc clusters are invariant under cubic symmetry operations. On the other hand, because the center spin must remain fixed under all symmetry operations, the symmetry group is necessarily a point group. However, the largest point group, known as $O_h$, is the full symmetry group of the cube. Therefore, the symmetry group of the cube is the largest possible symmetry group of these clusters. The main advantage of considering the symmetry groups is in finding the degeneracy factors of different geometries. For small clusters with complete shells, the empty sites at the next shell all have the same coordination number. For the bcc structure, as described earlier, this holds up to clusters with several hundred spins, while in the fcc lattice situation gets complicated already for small clusters due to the fact that atoms within the outermost shells can be nearest neighbors to each other. We have classified the geometries for fcc and bcc clusters and calculated their geometrical degeneracies.

As an example, for FCC-25 the maximum coordination criterion yields three geometrically different configurations with degeneracy factors 3, 3, and 1. If the clusters are produced in a way that the ratio of the abundances of these three geometries is determined by cohesion only, the magnetization is simply a weighed average of these three configurations. In Fig. 4 we show the resulting average magnetization together with the magnetization of the three geometrical isomers at two temperatures. Evidently, magnetization has a stepwise structure similar to that of clusters with complete shells. Due to the three different geometrical configurations, extra steps resulting from each individual geometry appear at low temperatures. From Fig. 4 we observe that this effect of geometrical degeneracy disappears rapidly for increasing temperature.

However, some qualitative features can be determined by the underlying crystal structure.[10,16,17] One such property turns out to be the size dependence of magnetization. This is demonstrated for fcc and bcc lattices in Fig. 5, where we show magnetization in the presence of an external field as a function $N$. For the chosen values of $B$, the size dependence of $M$ is indeed very different for fcc and bcc clusters. This

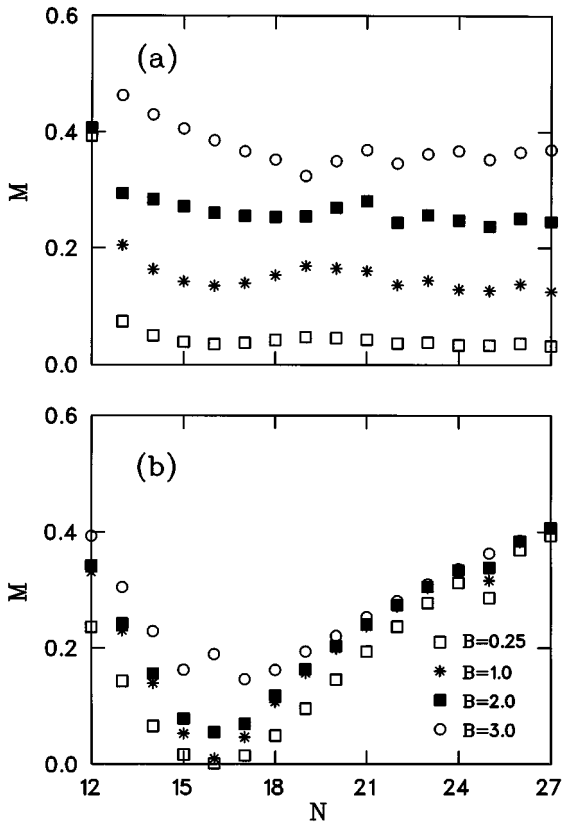


FIG. 5. Magnetizations of (a) fcc and (b) bcc clusters in four different applied fields at temperature T=1.0.

provides an indirect method to determine the crystal structure from the observed macroscopic behavior. However, we note that the characteristic features of magnetization for each structure can also depend on $T$.

Qualitative differences between the magnetic properties of fcc and bcc clusters also appear in their dependence on the average coordination number $c$. This is most clearly seen at low temperatures with a low but nonzero external magnetic field. This is the case in Fig. 6, where we show the ratio of total magnetization $NM$ and $c$ as a function of $c$ for fcc and bcc clusters with $N=12,\ldots,27$ for $T=0.2$ and $B=0.5$. For these values, the low-lying and possibly highly degenerated excited states have practically no influence on magnetization. The magnetization $NM$ of the fcc clusters turns out to be approximately proportional to $c$. In the fcc structure with increasing $c$, more frustration[10] is induced, which results in that more spins are able to align themselves with the external field, and this explains the observed behavior. For bcc clusters with $N=12,\ldots,16$, i.e., for increasing filling of the third shell, $NM/c$ decreases with increasing $N$, dropping to almost zero for BCC-16. Then it increases rapidly up to the cluster with $N=27$, which has complete shells again. However, at the same time the coordination number decreases monotonically from 4.25 for BCC-16 to 4.15 for BCC-27. With bcc clusters with $N\leqslant 9$ (data not shown), the magnetization monotonically increases as a function of coordination, when the second shell (the first shell being the center spin) is filled, which is easy to understand because the added spins are coupled only to the spin in the center. We can then conclude that it is not the average coordination but the size and geometry of the cluster which dominate in bcc clusters, while the magnetization of fcc clusters is mainly determined by the average coordination number.

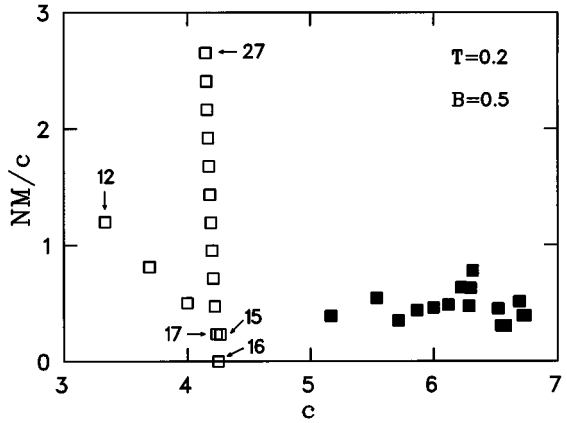


FIG. 6. Total magnetization $NM$ per average coordination number $c$ as a function of $c$ for bcc (open squares) and fcc (filled squares) clusters of sizes from 12 to 27 atoms at temperature $T=0.2$.

The qualitative differences between the trends in magnetic behavior of fcc and bcc clusters for increasing $N$ can be understood by considering the detailed structure of magnetic ordering. A crucial difference is that in bcc clusters atoms never have nearest neighbors within the same shell. Therefore, because $N$ is increased by adding one spin at a time at a given shell into a similar environment, the effects due to subsequent new spins add up. In fcc clusters the opposite is true: Spins within a given shell have nearest-neighbor couplings between them, and due to the criterion of maximum cohesion used in building these clusters, new atoms are preferentially added into locations where there already are neighbors within the same shell. This leads to a smaller magnetization for fcc clusters than for bcc clusters at low temperatures and in weak external fields, which is also consistent with the qualitative conclusions on the role of frustration in Ref. 10.

## V. EFFECTS OF LOCALLY MODIFIED COUPLING STRENGTHS

In real clusters the strength of the magnetic interaction between two spins is related to the overlap of electron wave functions.[11] Supposedly this overlap is smaller on the *surface* than in the bulk. To study the possible effect of this on the observed magnetic properties, we have first generalized our model to a case in which the coupling parameter $J_{ij}$ between surface and core spins is smaller than between core spins. For small clusters, it is reasonable to define a ''surface atom'' as one with the coordination number smaller than the average coordination of the cluster. With the cluster sizes considered in this work, for fcc clusters about a half and for bcc clusters more than a half of the atoms are surface atoms. Then we set the coupling strength $J_{ij}$ between the surface and the core atoms to be 2/3 of the core value. The results (not shown here) for clusters with both complete and incomplete shells are qualitatively very similar to the cases described above. As expected, in some cases extra steps appear

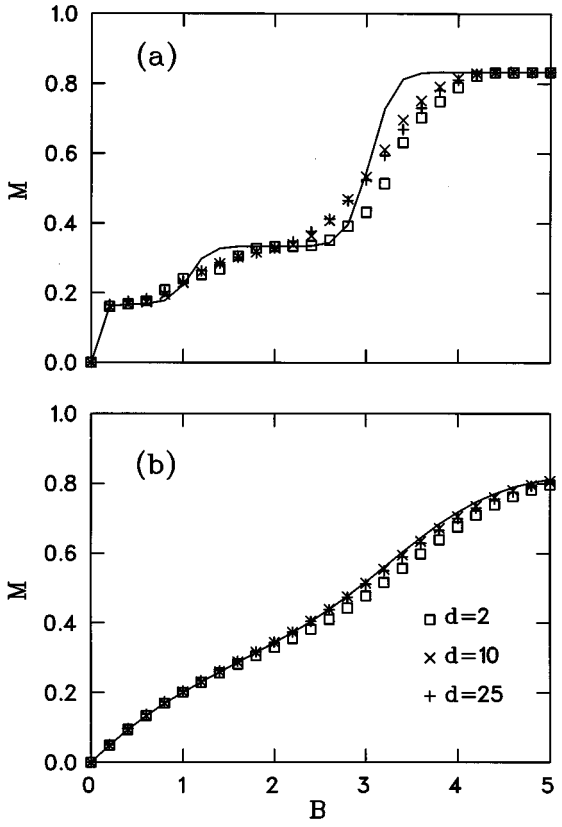


FIG. 7. Magnetization of the fcc cluster with 12 spins averaged over $d=$ 2, 10, and 25 different random sets of couplings compared with the magnetization of the nonrandomized FCC-12 cluster (solid curve) at temperatures (a) $T=0.2$ and (b) $T=1.0$.

in the magnetization curves, partly due to the ''incommensurate'' value 2/3 chosen here. Also, the role of surface spins as described in previous sections is more prominent due to the softer coupling with the core spins.

Next we consider a more general case in which $J_{ij}$ is allowed to vary *randomly*. The physical picture behind this possibility is that due to various relaxation processes, small clusters do not necessarily have the exact symmetry of any Bravais lattice.[16,18] Thus because of the varying nearest-neighbor distances, the value of $J_{ij}$ is expected to vary within a cluster. For this study, we chose two possible values for $J_{ij}$ differing from each other by a factor of 2/3. The choice of only two possible values makes the numerical work based on the algorithm described in Sec. II easier without affecting our main conclusions. Now the thermodynamic averages have to be calculated over different realizations of this *frozen disorder*. Notice that the coupling structure and the coordination numbers of spins within a given geometry remain unchanged. For clusters with incomplete shells, we then have to average also over the different geometrical isomers as described in Sec. IV. The magnetic properties of these clusters were calculated in such a way that a certain number, to be denoted by $d$ below, of randomly picked realizations $\{J_{ij}\}$ of coupling disorder for each geometrical isomer was generated. The final observed magnetization is then the properly weighted average over all these isomers. Typical magnetization curves are shown in Fig. 7, where the plotting symbols denote results for various values of $d$, and the solid lines show the results for the corresponding nonrandomized cluster. We can conclude that the overall structure of the magnetization isotherms is not affected by random couplings after all averages are done. This is consistent with the result in Ref. 16 that small distortions of the geometry of the $Ni_{13}$ cluster do not change the level structure of low-lying states. Another observation from Fig. 7 is that the extra steps in the $M=M(B)$ curves of individual realizations of the randomness disappear for increasing $d$ already at quite low temperatures, and the convergence of $M$ as a function of $d$ is quite rapid. We find that both fcc and bcc structures are rather insensitive to random couplings in this sense.

The general picture obtained from above indicates that magnetic properties for a given geometry can be predicted without exact knowledge about individual coupling strengths. This rather encouraging result can be interpreted in the following way. Two clusters with different sets $\{J_{ij}\}$ but with same $N$ can actually be considered as two different geometrical forms. However, this differs from the case of clusters with incomplete shells discussed in Sec. IV in that the number of ''acceptable'' isomers is much larger here. Therefore, fluctuations due to the randomness can be smoothened out already at relatively low temperatures. Based on the geometrical interpretation of $\{J_{ij}\}$, we can also conclude that this should also be the case for more general random couplings than the binomial distribution used above.[19]

## VI. FRUSTRATION AND THE SUPERPARAMAGNETIC MODEL

Besides the usual high-temperature paramagnetism,[11] in finite *ferromagnetic* clusters a completely different phenomenon, superparamagnetism, has been observed.[1–3] At low temperatures a ferromagnetic cluster can appear as a single giant paramagnetic spin, formed by the atomic magnetic moments ferromagnetically aligned to produce the total magnetic moment of the cluster. In the case of free clusters, rotation of this paramagnetic spin is made possible by coupling via magnetic anisotropy of the spin angular momentum to cluster rotations.[2] For an Ising ferromagnet this kind of superparamagnetism leads to magnetization

$$M=\frac{\mu}{N}\tanh\left(\frac{B\mu}{kT}\right), \tag{6.1}$$

where the effective total magnetic moment $\mu$ of the cluster is well approximated[20] by $\mu(T)\approx N|M|_{T,B=0}$. For a cluster of classical Heisenberg spins the corresponding magnetization is given by the Langevin function.[2]

The tanh function of Eq. (6.1) is of course a result of the two-state nature of an Ising system, and it is obvious how *antiferromagnetic* Ising clusters could in principle produce similar kind of behavior. Consider first a nonfrustrated system with nearest-neighbor antiferromagnetic couplings on a bipartite lattice structure which can be decomposed into two interpenetrating sublattices A and B (e.g., the bcc structure). At very low temperatures with $T,B\ll|J|$, the two sublattices are magnetized in opposite directions. In a finite system it can happen that the number of spins in the two sublattices differ, i.e., $N_A\neq N_B$, which leads to net magnetization at low

TABLE II. Configurations of lowest energies at $B=0$ for four small Ising clusters with complete shells and $J_{ij}\equiv J$. The last column $n(\epsilon_r,m_r)$ shows the number of configurations with energy $\epsilon_r$ (in units of $|J|$) and magnetization $m_r/N$. For the cluster OCT-6 all configurations are listed.

| Cluster | $\epsilon_r$ | $m_r$ | $n(\epsilon_r,m_r)$ |
|---|---|---|---|
| BCC-15 | $-32$ | $\pm1$ | 1 |
| | $-24$ | $\pm1,\pm3$ | 8,6 |
| | $-20$ | $\pm1$ | 24 |
| BCC-27 | $-56$ | $\pm11$ | 1 |
| | $-52$ | $\pm9$ | 12 |
| | $-48$ | $\pm7,\pm9$ | 66,6 |
| FCC-19 | $-20$ | $\pm1,\pm3,\pm5$ | 48,21,3 |
| | $-18$ | $\pm1,\pm3$ | 308,84 |
| | $-16$ | $\pm1,\pm3,\pm5$ | 1014,300,12 |
| OCT-6 | $-4$ | $0,\pm2$ | 12,3 |
| | 0 | $0,\pm2$ | 8,12 |
| | $+4$ | $\pm4$ | 6 |
| | $+12$ | $\pm6$ | 1 |

temperatures. For an Ising antiferromagnet there would be in this case two dominating configurations with a total magnetic moment $\mu\approx|N_A-N_B|$. Two such examples, the clusters BCC-15 and BCC-27 with $\mu\approx|m_r|=1$ and $\mu\approx11$, respectively, can be found in Table II. In the ferromagnetic case Eq. (6.1) is a surprisingly good approximation up to temperatures a few times the coupling constant.[20] For Ising antiferromagnets the situation is different, however. For ferromagnets in the superparamagnetic region, the length of the superparamagnetic ''spin'' is $\mu\approx N$, whereas for antiferromagnets it is considerably lower, roughly proportional to the surface area of the cluster. Thus, for the latter, thermally excited single spin flips can result in a much larger relative change in the total magnetic moment of the cluster, and consequently, a clear deviation from the low-temperature superparamagnetic magnetization occurs much earlier.

In Fig. 8 we show the behavior of the central quantity of an Ising superparamagnet, $|M|$ at $B=0$, as a function of temperature for six small antiferromagnets. It is evident that no simple and coherent behavior can be found in this case of antiferromagnets. It is even impossible to tell apart frustrated (ico,fcc,hcp) and nonfrustrated (bcc) structures. The qualitative features of the curves in Fig. 8 can, however, be explained. The increase of $|M|$ with increasing temperature, beginning at intermediate temperatures, is a result of the increase of disorder with increasing temperature. Disorder counteracts the tendency of the antiferromagnetic order to reduce the net magnetic moment of the cluster. The behavior at low temperatures, on the other hand, is determined by the detailed structure of the configurations with lowest energies. For the cluster BCC-15, e.g., the absolute magnetization of the ground state ($\epsilon_r=-32$) is, from Table II, $|M|=|m_r|/N=1/15$. With increasing temperature excited states become noticeable, first those with $\epsilon_r=-24$ and $m_r=\pm1,\pm3$, which means that the absolute magnetization increases with temperature.[21] For the cluster BCC-27, an opposite situation occurs. The magnetization of the first excited states ($m_r=\pm9$) is lower than that of the ground state ($m_r=\pm11$), which leads to decreasing $|M|$ with increasing temperature.

We shall next consider the *frustrated* cases at low temperatures and in weak external fields. The sensitivity of the magnetic properties to lattice structure became obvious while discussing the Fig. 2 in Sec. III. Interestingly, the clusters FCC-13 and HCP-13 are expected to behave like superparamagnets because of the simplicity of their ground states at $B=0$: for these clusters one finds from Table I that $m_r=\pm3$ and $m_r=\pm1$, respectively. The fact that the number of such configurations, $n(\epsilon_r,m_r)$, is different from unity has no consequences on Eq. (6.1). Notice that in Figs. 2(b) and 2(c) the difference by a factor of 3 between the two

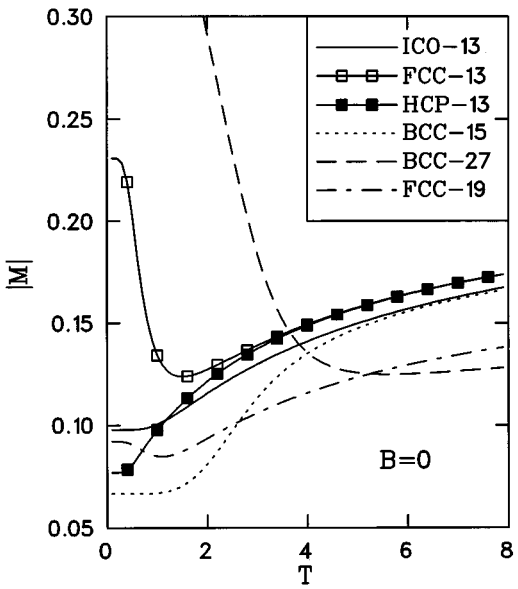


FIG. 8. Absolute magnetization $|M|$ at $B=0$ for six small Ising clusters as a function of temperature $T$.

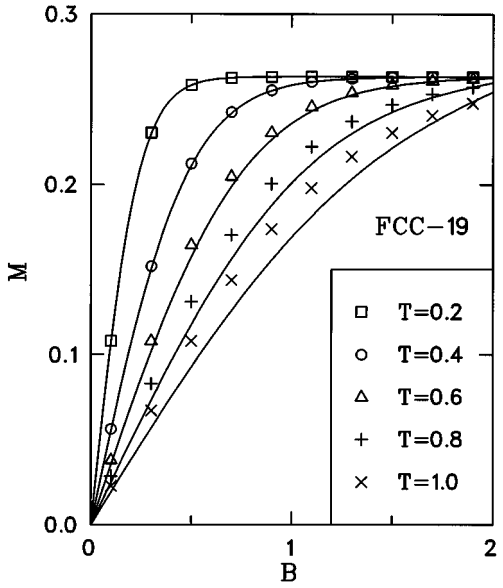


FIG. 9. Magnetization of the Ising cluster FCC-19 as a function of the external magnetic field $B$. The solid curves show the exact averages over all configurations and the plotting symbols denote the low-temperature approximations given by Eq. (6.3).

effective $\mu$'s as given by $m_r$'s can directly be seen in the slopes near $B=0$ of the respective magnetization curves for $T=0.5$. Despite the fairly similar geometries of these two clusters, the response to an external field $B$ of HCP-13 is, because of the value of $\mu$, closer to that of ICO-13 [see Fig. 2(a)] than to that of FCC-13. However, from Table I, ICO-13 has a more complicated ground state at $B=0$ which has $m_r=\pm 1,\pm 3$. Therefore the functional form of $M$ is not given by tanh in this case.

When another shell of atoms is added to FCC-13, FCC-19 is formed. This cluster can no more be regarded as a simple superparamagnet: From Table II, its partition function can be approximated at low temperatures and small external fields by taking into account the configurations with $\epsilon_r=-20$, with the result

$$Z_{\text{FCC-19}} \approx e^{20J/kT}[3x^5+21x^3 + 48x+48x^{-1}+21x^{-3}+3x^{-5}], \qquad (6.2)$$

where $x=\exp(B/kT)$. From this the magnetization of FCC-19 is given by

$$M_{\text{FCC-19}} \approx \frac{1}{57}\tanh\left(\frac{B}{kT}\right)\left[13+\frac{4\sinh^2(B/kT)}{3+2\sinh^2(B/kT)}\right] \sim \frac{13}{57}\frac{B}{kT}+O((B/kT)^3). \qquad (6.3)$$

In Fig. 9 the result, Eq. (6.3), is compared with the result of a brute force calculation over all significant states shown by the solid lines. As expected, agreement between the results is excellent at lowest temperatures. However, a clear deviation from the exact result is observed already at $T=0.6$. The reason for this early deviation is readily seen from Table II: The difference in the coupling energy $\epsilon_r$ between the states taken into account in Eq. (6.2) and the lowest excited states that have been neglected is only $\Delta\epsilon=2$. This corresponds to reversing the sign of the coupling energy of one pair of nearest neighbors. The effect of the omission of these configurations is further amplified by their contribution to entropy which reflects their relatively high values of $n(\epsilon_r,m_r)$ due to frustration. Notice that the tanh function in Eq. (6.2) has nothing to do with the simple superparamagnetic description; in this case it results from three different values of the effective magnetic moment ($\mu=1,3,5$).

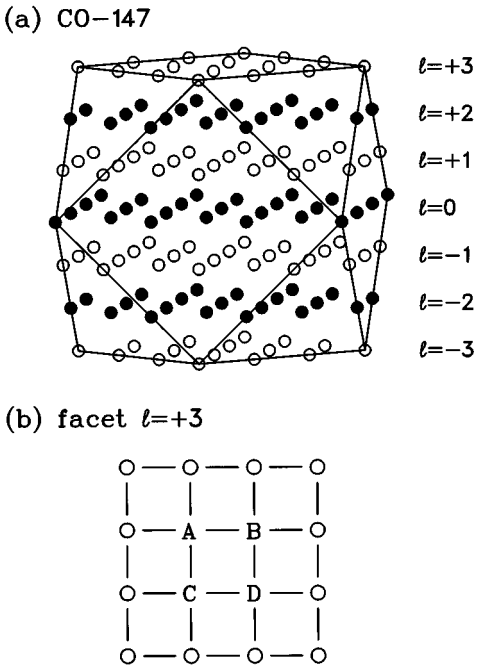


FIG. 10. (a) Ground-state configuration at $B=0$ of the cuboctahedron with $N=147$ spins. Open circles denote spins with $S_i=+1$ and solid circles those with $S_i=-1$. (b) Ordering of the fcc(100) facet formed by the atoms in the layer $\ell=+3$.

In addition to the data shown here, we have done similar analysis of other cluster geometries with consistent conclusions. For antiferromagnets in general, the energy cost (in units of $J$) of single spin excitations is, due to frustration, lower for close-packed (fcc), and otherwise densely packed (ico) structures, than for more loosely packed (e.g., bcc) structures. This is of course in contrast with the ferromagnetic case.

One case of special interest is the cuboctahedral cluster geometry[12] with the fcc close-packed lattice structure. The number of atoms in such clusters with complete shells, as defined in Ref. 13, can have values $N=13,55,147,309,\ldots$ . In Fig. 10(a) we show the conjectured ground-state configuration of the Ising antiferromagnet CO-147. This state consists of alternating ordered layers in the (100) direction, within which the spins are aligned either ''up'' or ''down,'' which is exactly the structure of the ground state of the fcc *bulk* Ising antiferromagnet at $B=0$. For the cuboctahedra, however, the ground state is highly degenerate. First, there is the usual degeneracy arising from the cubic symmetry. Second, in the middle of the topmost and lowermost (100) facets there are spins that can flip ''almost freely'': They are denoted by letters A–D in Fig. 10(b). They have four nearest neighbors in their own positively magnetized ($S_i=+1$)

layer $\ell=3$ and other four nearest neighbors with $S_i=-1$ in the layer $\ell=2$. Thus, any of the spins A–D can be reversed without cost in energy, if their neighbors within the same layer have $S_i=+1$. This means that, at $B=0$ and at a time, up to four spins can be reversed at two opposite facets of this cluster, without cost in energy. Of course, it is not possible to verify this conjecture for the ground state by going through all the $2^N$ spin configurations, but we have checked it for cuboctahedra of sizes $N=55$–$309$ by a standard simulated annealing procedure[14] with a total simulation length of $10^8$ Metropolis steps per spin. These simulations easily reach the bulklike configurations, but none have been obtained with a lower energy. Also, it is easy to verify by simple bond-counting arguments that, if the ground state is bulklike, there must be ''free'' spins just as described above. Thus, in a cuboctahedron with $N\geqslant 55$, there does exist (cf. Ref. 10) free spins at $B=0$, surprisingly not on the ''frustrated'' triangular (111) facets but on the (100) facets. The cluster CO-13 (FCC-13) is an exception because of the small size of these facets.

For the clusters with fcc lattice structure, we conclude that at low temperatures and in weak applied fields, already for relatively small cluster sizes the behavior is that of the bulk antiferromagnet modified by surface effects. In Sec. VII we give some more evidence that the ground-state spin configuration of even a 14-atom cluster resembles very much the bulk configuration. However, it is the surface effects which produce the observed *net* magnetization, and this makes the behavior somewhat unpredictable. In the case of the cuboctahedral shape, the surface spins (which here means the spins not quenched to the bulk order) are divided into two independent domains on facets on the opposite sides of the cluster. For other geometries, there are cases in which the surface spins form a connected net which spreads over the whole cluster. This net can be either strongly connected, or it can consist of domains only weakly (through one spin) connected with each other. Therefore, no generic ''phase diagram'' can be constructed in the antiferromagnetic case.

## VII. FINITE-SIZE TRANSITIONS

We have also investigated possible ''phase transitions'' in these finite systems by calculating absolute magnetization of different shells of the cluster and in the case of bcc clusters also the sublattice magnetization. Typical results for the sublattice magnetization of bcc clusters are shown in Fig. 11(a). The first zero of the second derivative or the turning point of the magnetization curve can be considered as the point separating the ordered antiferromagnetic phase from the disordered paramagnetic phase. As expected, this point, known as the Néel temperature in the bulk limit, is shifted towards higher temperature with increasing system size. In fcc clusters the situation changes to some extent, as seen from Fig. 11(b). The difference between the Néel temperatures of clusters FCC-14 and FCC-27 is considerably smaller than that for bcc clusters of the same sizes, almost negligible. This is consistent with the conclusion made in Sec. VI that, at low temperatures, the magnetic ordering at the innermost shells is very similar to that in an infinite fcc lattice already for very small clusters. As mentioned above, the results shown here are typical of all small clusters considered in this work.

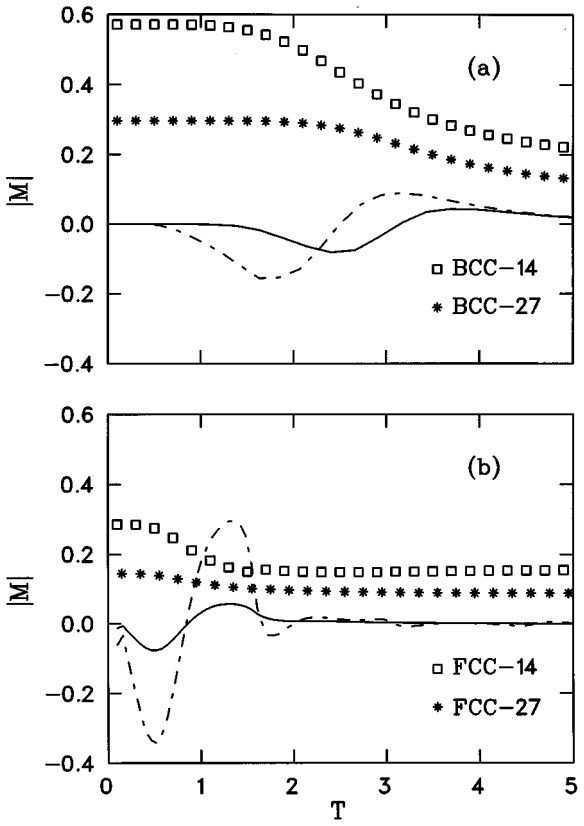


FIG. 11. Absolute magnetizations of (a) BCC-14 and BCC-27 and (b) FCC-14 and FCC-27 clusters at temperature $T=1.0$. The second derivatives of the magnetization curves of clusters with 14 and 27 atoms are shown with dashed and solid lines, respectively.

We have demonstrated that, in these finite-size systems, it is possible to speak of a ''transition'' temperature which, in the thermodynamic limit, approaches the usual Néel temperature. In this case a sharp transition is replaced by a rounded cross-over, but it is, however possible to speak about a low-temperature ordered phase and a high-temperature disordered or paramagnetic phase, as we have done in previous sections. The ordered phase of antiferromagnetic spin clusters is characterized by a stepwise structure of magnetization as a function of the external field. Finite-size effects on magnetic transitions have extensively been studied,[17,18,22–24] and it is not necessary to discuss them in more detail here. We only notice that real clusters exemplify systems for which the introduction of the concept of *finite-size transitions* seems indeed very proper.[25]

## VIII. DISCUSSION AND CONCLUSIONS

We shall now briefly discuss the experimental relevance of our results. In the ferromagnetic case, it has been shown earlier that Ising model is able to provide a reasonably good qualitative description of some phenomena like superparamagnetism as observed in the experiments. However, it is well known that the difference between the Ising description and real quantum interactions is much more pronounced in the antiferromagnetic than in the ferromagnetic case. For example, the ground state of a Heisenberg antiferromagnet does not usually have a simple correspondence with that of a system with classical spins.[11,26] To consider this point, we

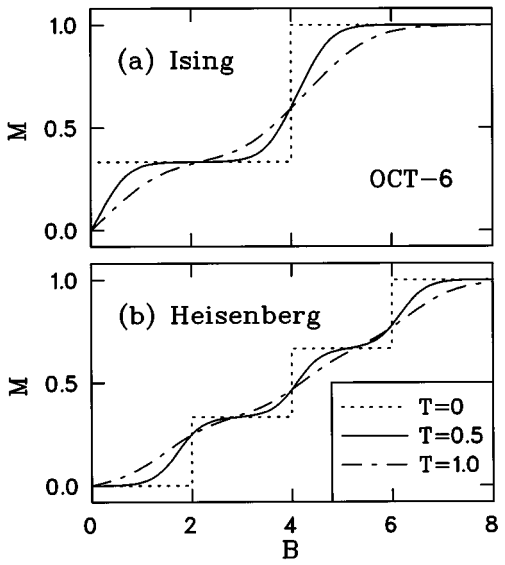


FIG. 12. Magnetization as a function of the external magnetic field $B$ of the cluster OCT-6 for the (a) Ising model and (b) spin-1/2 Heisenberg model. In (b), the units have been chosen to coincide with those of the Ising model.

have studied a few small spin-1/2 Heisenberg clusters. A typical result is shown in Fig. 12. For the octahedron with $N=6$, the main effect of including the $S_x$ and $S_y$ components in the model seems to be to double the steps in the magnetization curves. The characteristic features of the antiferromagnetic case remain the same: The ground state can change as a function of the external field, and for $B\neq 0$ the magnetization is not necessarily a monotonic function of temperature. For many geometries some of the steps in magnetization isotherms are doubled, in some cases they are only shifted to a different value of $B$. Also, it is evident that at very low temperatures and in small applied fields the direction of magnetization of real clusters is determined by lattice anisotropy like in bulk magnetism. This is true for ferromagnetic[1] and antiferromagnetic clusters alike. However, very much as in the ferromagnetic case,[1] there is an antiferromagnetic blocking temperature above which thermal energy exceeds the magnetic anisotropy energy. Therefore, above this blocking temperature, the direction of (sublattice) magnetization can freely rotate with respect to the lattice structure, and both Ising and Heisenberg models should provide an adequate qualitative description.

For a complete description of magnetic properties, one should naturally first calculate the ground state geometry of the cluster and actually carry out a full calculation of the electronic structure.[3] Due to relaxation processes, the cluster is not expected to have the ideal symmetry of a crystal lattice in most cases. An obvious consequence would then be that the structure of energy levels (for the magnetic degrees of freedom) becomes more complicated. One would therefore expect more steps in the $M(B)$ curves. A similar effect would also result from the fact that in realistic situations several structural isomers can coexist. However, as shown in this work, these complications do not seem to change the properties of antiferromagnetic clusters in a qualitative way. In particular, within a given model for a known lattice structure, the magnetic behavior is not strongly dependent on the details of the set of exchange energies $\{J_{ij}\}$, which makes possible even quite crude approximations to the corresponding exchange integrals. This indicates that qualitative thermodynamic properties of small antiferromagnetic clusters could reasonably well be described by suitably chosen spin Hamiltonians, for which the coupling parameters can be obtained from first-principles calculations if desired.

To summarize, we have considered in detail the magnetic properties of small antiferromagnetic clusters within the framework of the nearest-neighbor Ising model. For external fields large compared with the strength of the coupling between spins, we observe a step-wise structure of magnetization, which results from field-induced transitions in the internal magnetic order of a cluster. In the presence of a finite external field, we also find that magnetization can be an increasing function of temperature for a considerable temperature range. These features were found, at low temperatures, to strongly depend on the lattice structure of the clusters, but can be understood by examining the lowest-lying excited states in each case. Within each lattice structure, even for nonideal structures, the magnetic properties were found to be rather robust against local modifications of the strength of the antiferromagnetic couplings between spins. We also examined the possibility of observing low-temperature superparamagnetism in the antiferromagnetic case. Concerning antiferromagnetic ordering, we found that, despite the considerable finite-size effects, clusters as small as 20 spins can display bulklike thermodynamic properties. We would expect that our main conclusions will hold for clusters of at least several tens of spins even though most of the computations were only performed for clusters with less than 30 spins. However, we find no simple general scheme for antiferromagnets, like the one the superparamagnetic model provides for the present understanding of the experimental results on ferromagnetic clusters. An intriguing observation is that it seems possible to distinguish between different crystal structures from the dependence of magnetization on the atomic number of the cluster, i.e., from observable macroscopic properties.

## ACKNOWLEDGMENTS

This work has been supported by the Academy of Finland and the University of Jyväskylä. One author (J.M.) also thanks the Emil Aaltonen Foundation for financial support.

[1] For a review on ferromagnetism in small clusters, see J. P. Bucher and L. A. Bloomfield, Int. J. Mod. Phys. B **7**, 1079 (1993).

[2] S. N. Khanna and S. Linderoth, Phys. Rev. Lett. **67**, 742 (1991).

[3] S. N. Khanna and P. Jena, in *Physics and Chemistry of Finite Systems: From Clusters to Crystals*, edited by P. Jena, S. N. Khanna, and B. K. Rao (Kluwer, Dortrecht, 1992), Vol. I.

[4] S. E. Apsel, J. W. Emmert, J. Deng, and L. A. Bloomfield, Phys. Rev. Lett. **76**, 1441 (1996).

[5] W. A. de Heer, P. Milani, and A. Châtelain, Phys. Rev. Lett. **65**, 488 (1990).

[6] J. P. Bucher, D. C. Douglass, and L. A. Bloomfield, Phys. Rev. Lett. **66**, 3052 (1991); J. P. Bucher, D. C. Douglass P. Xia, B. Haynes, and L. A. Bloomfield, Z. Phys. D **19**, 251 (1991).

[7] P. Milani and W. A. de Heer, Phys. Rev. B **44**, 8346 (1991); M. L. Billas, J. A. Becker, and W. A. de Heer, Z. Phys. D **26**, 325 (1993).

[8] A. J. Cox, D. C. Douglass, J. G. Louderback, A. M. Spencer, and L. A. Bloomfield, Z. Phys. D **26**, 319 (1993).

[9] J. P. Bucher and L. A. Bloomfield, Phys. Rev. B **45**, 2537 (1992).

[10] B. V. Reddy and S. N. Khanna, Phys. Rev. B **45**, 10 103 (1992).

[11] N. W. Ashcroft and N. D. Mermin, *Solid State Physics* (Holt, Rinehart and Winston, New York, 1976); D. C. Mattis, *The Theory of Magnetism I,II* (Springer, Berlin, 1981).

[12] B. Raoult, J. Farges, M. F. De Feraudy, and G. Torchet, Philos. Mag. B **60**, 881 (1989); C. L. Cleveland and U. Landman, J. Chem. Phys. **94**, 7376 (1991); H-P. Cheng, R. S. Berry, and R. L. Whetten, Phys. Rev. B **43**, 10 647 (1991); S. Valkealahti and M. Manninen, *ibid.* **45**, 9459 (1992).

[13] T. P. Martin, Phys. Rep. **273**, 199 (1996).

[14] E. Aarts and J. Korst, *Simulated Annealing and Boltzmann Machines* (Wiley, Chichester 1989).

[15] D. W. Heermann, *Computer Simulation Methods in Theoretical Physics* (Springer, Berlin, 1986).

[16] F. A. Reuse, S. N. Khanna, and S. Bernel, Phys. Rev. B **52**, 11 650 (1995).

[17] H. Cheng and L-S. Wang, Phys. Rev. Lett. **77**, 51 (1996).

[18] B. Piveteau, M-C. Desjonquéres, A. M. Olis, and D. Spanjaard, Phys. Rev. B **53**, 9251 (1996).

[19] Similar behavior of ferromagnets has been described in S. M. Zheng, Phys. Rev. B **52**, 7260 (1995).

[20] J. Merikoski, M. Manninen, and J. Timonen, in *Physics and Chemistry of Finite Systems: From Clusters to Crystals*, edited by P. Jena, S. N. Khanna, and B. K. Rao (Kluwer, Dortrecht, 1992), Vol. I.

[21] The feature that the first excited states can have a larger magnetization than the ground state has been observed, e.g., in the calculations of Ref. 16 for $Ni_{13}$ clusters.

[22] D. P. Pappas, A. P. Popov, A. N. Anisimov, B. V. Reddy, and S. N. Khanna, Phys. Rev. Lett. **76**, 4332 (1996).

[23] M. R. Scheinfein, K. E. Schmidt, K. R. Heim, and G. G. Hembree, Phys. Rev. Lett. **76**, 1541 (1996).

[24] G. M. Pastor, R. Hirsch, and B. Mühlschlegel, Phys. Rev. B **53**, 10 382 (1996).

[25] R. S. Berry, in *Large Clusters of Atoms and Molecules*, edited by T. P. Martin (Kluwer, Dortrecht, 1996).

[26] The similarity between the ferromagnetic Ising and Heisenberg models is particularly evident in the superparamagnetic region (Ref. 20).